Integrating Satellite Remote Sensing and Dynamic GIS for Urban Flood Risk Modelling in Ulaanbaatar City

Erkhemzorig Ishdorj^{1,4}, Ochirkhuyag Lkhamjav^{2,3,4}, Ulziisaikhan Ganbold^{1,4*}

⁴ Mongolian Geospatial Association, Ulaanbaatar 15141, Mongolia - info@geomedeelel.mn

Keywords: Flood risk assessment, GIS, remote sensing, weighted overlay model, Ulaanbaatar, climate change adaptation

Abstract

Climate change has intensified the frequency and severity of natural disasters globally. In Ulaanbaatar, Mongolia, rapid urbanization and high population density have heightened susceptibility to flood disasters, particularly those associated with extreme rainfall events. Historical data reveal a pronounced increase in flood occurrences, with 60% of the 45 recorded floods between 1995 and 2021 occurring from 2000 to 2009. The 2020 flood event alone breached levees at six locations and damaged 60 structures, underscoring the imperative for robust flood risk assessment and mitigation strategies. This study employs high-resolution remote sensing data within a GIS framework to conduct a comprehensive flood risk assessment. Diverging from conventional hydrological models (e.g., SWMM, HEC-RAS), an overlay weighted model is utilized for its efficacy in multi-criteria spatial analysis. Six parameters are integrated: land use/cover (LULC), elevation (12.5 m DEM), slope, watershed boundaries, flow direction, and precipitation (90 m resolution). Data sources include ALOS/PALSAR (DEM), Sentinel-2 (LULC), and CRU TS v4 (precipitation). Thematic analysis identifies Khan-Uul and Sukhbaatar districts as high-risk zones due to low-lying topography, while steep-sloped areas exhibit lower vulnerability. The risk map classifies 19.66% (775.7 km²) as "very high risk" (e.g., Tuul and Selbe riversides) and 25.5% (1,006.89 km²) as "high risk," corroborating historical events like the 1966 flood (103.5 mm rainfall, 43% of annual average).

1. Introduction

The frequency and intensity of natural disasters have exhibited significant escalation in recent decades, primarily attributed to anthropogenic climate change and global warming phenomena (Intergovernmental Panel on Climate Change, 2023) and (NASA, 2024). Among these disasters, flooding represents one of the most catastrophic natural hazards, resulting in substantial loss of life, extensive property damage, and critical infrastructure disruption, thereby affecting millions of individuals across the globe (Intergovernmental Panel on Climate Change, 2022).

Flooding can be conceptually defined as a hydrological phenomenon characterized by the rapid elevation of water levels resulting from intense precipitation events or accelerated snowmelt and ice ablation processes over compressed temporal periods, subsequently causing riverine overflow and inundation of adjacent lowland and coastal territories (Chebotarev, 1975). In addition to being caused by rainfall and melting snow and ice, floods can also be caused by natural phenomena such as earthquakes, landslides, and ice caps, as well as other man-made events such as dam failures (Maidment, 1992). The contemporary landscape of flood modeling research encompasses a diverse array of methodological approaches, including models based on hydrologic, hydraulic, numerical,

rainfall—runoff, remote sensing and GIS, artificial intelligence and machine learning, and multiple-criteria decision analysis (Kumar et al. 2022). The integration of hydraulic and hydrological modeling frameworks constitutes a fundamental prerequisite for comprehensive flood risk assessment and the development of evidence-based mitigation strategies (Dysarz et al. 2023). Through systematic analysis of hydrodynamic processes during flood events, researchers can identify areas of elevated flood susceptibility and quantify potential impacts, including structural damage to build environments, infrastructure degradation, and human casualty risks (Bruno et al. 2022). This analytical foundation serves to inform both structural and non-structural risk reduction strategies while supporting comprehensive emergency response planning protocols (Figure 1).

Urban environments face perpetual flood vulnerability due to the extensive presence of impervious surfaces that fundamentally alter natural hydrological processes (Chen et al. 2020) and (Li et al. 2025). Research demonstrates that impervious surface percentage exhibits the strongest explanatory ability (69.58%) for urban water runoff, significantly surpassing other factors such as mean annual precipitation (15.51%), GDP (14.03%), and population density (11.98%) (Chen et al. 2020). Ulaanbaatar, Mongolia's capital city, exemplifies the challenges faced by

¹ School of Geology and Mining Engineering, Mongolian University of Science and Technology, Ulaanbaatar 14911, Mongolia – <u>ierkhemzorig@gmail.com</u>, <u>ulziis@must.edu.mn</u>

² Department of Civil Engineering, National Central University, Taoyuan 32017, Taiwan (ROC) - <u>olkhamjav@g.ncu.edu.tw</u>
³ Institute of Geography and Geoecology, Mongolian Academy of Sciences, Ulaanbaatar 15170, Mongolia – <u>ochirkhuyag 1@mas.ac.mn</u>

rapidly urbanizing areas in managing stormwater infrastructure. The city's urban development trajectory commenced with the adoption of a comprehensive general plan in 1954, followed by the systematic implementation of stormwater drainage infrastructure in 1960 and flood protection measures in 1966 (Asian Development Bank, 2018). Recent infrastructure assessments indicate that Ulaanbaatar has constructed five flood protection and drainage facilities, providing flood protection benefits to over 27,000 residents and improved sanitation infrastructure to 6,000 individuals, with indirect benefits extending to approximately 1 million people across the capital (Climate Change News, 2022). Currently, Ulaanbaatar's stormwater drainage network encompasses 169 kilometers of infrastructure with 3,388 access points; however, critical infrastructure assessment reveals that more than 80% of the primary drainage network has reached the end of its operational lifespan and requires comprehensive renovation (World Bank, 2020)

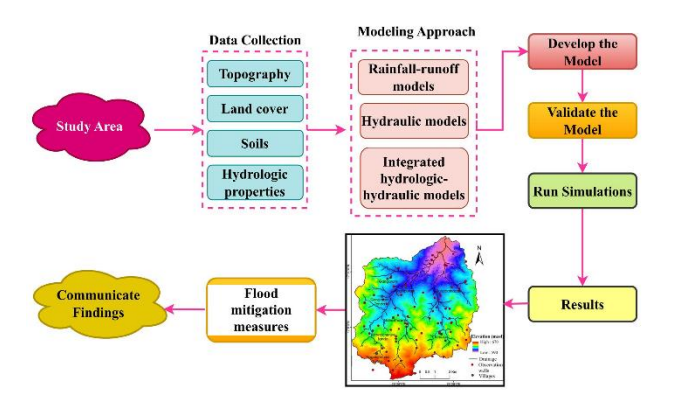


Figure 1. Stages of hydrological and hydraulic modeling

[Source: Kumar et al. 2022]

The exponential demographic growth in Ulaanbaatar's residential areas has coincided with increasing flood disasters precipitated by extreme meteorological events and intensified precipitation patterns, necessitating comprehensive risk assessment, spatial mapping, and vulnerability analysis (Al-Omari et al. 2024). Contemporary research demonstrates that remote sensing (RS) and Geographic Information System (GIS) applications have become essential tools for flood disaster risk management over the past two decades (Amatebell et al. 2025). The primary objective of this investigation is to conduct quantitative and qualitative flood risk assessment for Ulaanbaatar through the integration of high-resolution satellite imagery and remote sensing data within a comprehensive GIS analytical framework. Multiple computational modeling approaches have gained prominence in spatial flood risk analysis, including advanced hydrological and hydraulic modeling platforms such as i-Tree Eco, Storm Water Management Model (SWMM), and Hydrologic Engineering Center's River Analysis System (HEC-RAS), among others (Chen et al. 2009) and (Rjeily et al. 2017). Recent developments demonstrate the effectiveness of coupled modeling approaches, such as integrated SWMM-HEC-RAS 2D models, for quantifying urban flood risk by combining hazard magnitude assessment with vulnerability analysis (Khatooni et al. 2025). For this investigation, a weighted average model utilizing multi-criteria decision analysis (MCDA) was employed for comprehensive suitability assessment. The methodological framework incorporated critical geospatial parameters including land use classification, topographic elevation, slope gradient analysis, watershed delineation, hydrological flow direction modeling, and precipitation distribution patterns.

The development of thematic cartographic representations utilized the highest available resolution datasets for land use classification, digital elevation modeling, and precipitation analysis, as remote sensing and GIS are recognized as efficient approaches for spatially predicting flood risk mapping (Farhadi and Najafzadeh, 2021). The proactive flood risk assessment of Ulaanbaatar facilitated the creation of comprehensive thematic maps representing various input parameters, thereby enabling evidence-based planning and prediction of future risk mitigation strategies. This approach aligns with established methodologies that derive flood-producing factors from integrated soil, slope, elevation, drainage density, and land use/land cover data (Hagos et al., 2022). Furthermore, the utilization of satellite-derived data provides significant advantages in terms of cost-effectiveness and temporal efficiency while delivering medium-scale thematic cartographic products suitable for comprehensive urban flood risk determination and management planning.

This study aims to utilize ALOS PALSAR satellite data within a Geographic Information System (GIS) framework (e.g., ArcGIS) to develop a comprehensive flood risk map of Ulaanbaatar City and conduct a detailed land use analysis of selected high-risk zones. To achieve this overarching goal, the following specific objectives are proposed:

- Assess the current flood risk conditions in Ulaanbaatar City by evaluating historical flood events, hydrological data, and existing mitigation measures.
- Compare and evaluate different flood risk assessment methodologies to determine the most effective approach for the study area.
- Process and analyze spatial datasets to generate highresolution thematic maps, including elevation, water flow accumulation, and land cover classification.
- Develop a GIS-based flood risk map of Ulaanbaatar City, identifying the most vulnerable districts and communes.
- Conduct a land use and land cover (LULC) analysis of selected flood-prone areas to assess urbanization patterns, infrastructure exposure, and potential mitigation strategies.

2. Study Area

Ulaanbaatar, the capital of Mongolia, occupies a strategically significant position within the Tuul River basin, situated in a mountainous depression surrounded by prominent peaks of the Khentii Range (Gordillo Fuertes, 2023). The city is positioned at the confluence of several major topographic features, including the Asralt Khairkhan Mountain (2,799 m elevation), representing the highest peak of the Khentii Range, and lies in the shadow of Bogd Khan Mountain (mean elevation 1,350 m) (WWF, 2024). The urban area is further enclosed by a series of prominent elevations: Chingeltei Mountain (1,949 m), Bayanzurkh Mountain (1,834 m), Bogd Khan Mountain (2,256 m), and Songinokhairkhan Mountain (1,652)m). collectively encompassing a total metropolitan area of 4,704.44 hectares.

The developed urban core of Ulaanbaatar is situated at elevations ranging from 1,260 to 1,350 meters above sea level, with the entire terrain exhibiting a northward-sloping gradient from the northern mountain ranges toward the Tuul River basin (Gordillo Fuertes, 2023). The Tuul River, spanning 148 kilometers through the metropolitan area, serves as the principal hydrological feature and primary source of water supply for the capital, which

accommodates over 40% of Mongolia's population and generates 60% of the national GDP (Gordillo Fuertes, 2023). The river system originates from the Asralt Khairkhan Mountain and receives contributions from multiple tributaries, including the Gachuurt, Terelj, Tolgoit, and Uliastain rivers.

The eastern Selbe River represents a secondary but significant hydrological system, originating from the foothills of the Khentii mountain range at Ikh Bayan Mountain. This watercourse creates an extensive river basin incorporating numerous smaller tributaries, including the Khandgait, Sharga Moryt, Selkh, Belkh, Chingeltei and Ganz Khudgiin rivers. The Selbe River, originating approximately 35 kilometers north of the urban center, confluences with the Tuul River from the western approach; however, urban development has resulted in the complete obstruction of its western tributary system.

Ulaanbaatar experiences a harsh continental climate characterized by extreme seasonal temperature variations, with the city recognized as having one of the world's most severe winter climates. The average air temperature in January reaches -26°C, while July temperatures average +17°C. Annual average temperatures have increased by 2.1°C since the 1940s (Batimaa et al. 2011). The regional climate exhibits an average annual relative humidity of 61%, with prevailing winds originating from north and northwest directions at an average annual velocity of 2.4 m/sec (Batimaa et al. 2011).

Long-term climate analysis indicates that over the past six decades, Ulaanbaatar has experienced an average temperature increase of approximately 2.0°C, exceeding the national Mongolian average of 1.8°C, a phenomenon attributed to rapid urbanization effects (Ministry of Environment and Tourism, 2023). This urbanization has resulted in significant environmental challenges, including air pollution from coalburning stoves in informal settlements during cold seasons, with Mongolia committing to reducing greenhouse gas emissions by 22.7% by 2030 (UNICEF Mongolia, 2024) and (Climate and Clean Air Coalition, 2024).

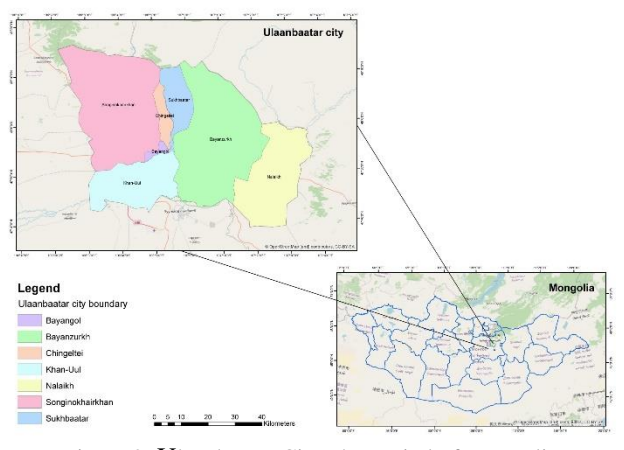


Figure 2. Ulaanbaatar City, the capital of Mongolia

The metropolitan area of Ulaanbaatar is administratively organized into nine distinct districts: Bayanzurkh, Bayangol, Songinokhairkhan, Chingeltei, Sukhbaatar, Khan-Uul, Nalaikh, Baganuur, and Bagakhangai. Three districts (Nalaikh, Baganuur, and Bagakhangai) are geographically separated from the central urban core (Figure 2). The spatial distribution of administrative districts demonstrates significant variation in area coverage: Bayanzurkh district encompasses 124,412 hectares, representing the largest administrative unit, followed by Songinokhairkhan

(120,063 hectares), Nalaikh (68,764 hectares), Baganuur (62,020 hectares), Khan-Uul (48,466 hectares), Sukhbaatar (20,840 hectares), Bagakhangai (14,000 hectares), Chingeltei (8,930 hectares), and Bayangol (2,949 hectares). Contemporary land use analysis of the unified metropolitan land fund reveals a predominant agricultural allocation, comprising 235,886.2 hectares (56.7% of total area). Urban, rural, and settlement areas account for 69,517.8 hectares (16.7%), while forest land encompasses 75,110.3 hectares (17.8%). Infrastructure allocation includes 6,019.6 hectares (1.4%) for transportation and utility networks, 4,078.2 hectares (1.0%) for water reservoir systems, and 26,082 hectares (6.3%) designated as special state land (National Statistics Office of Mongolia, 2022).

3.Approaches and Data set

Based on the comparison of the problems faced by countries in determining flood risk with the current situation of their own flood-prone areas, a workflow and methodology for spatial data analysis for determining flood risk were developed and analyzed accordingly (Figure 3).

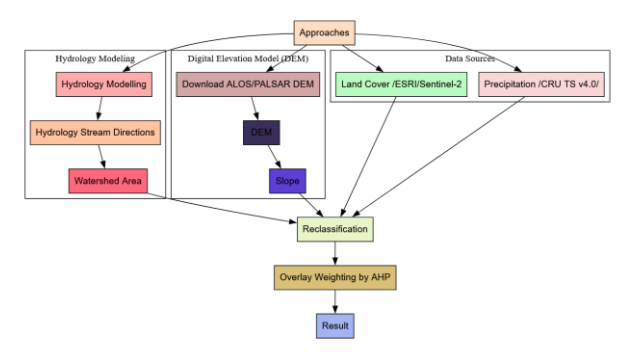


Figure 3. Research methodology flowchart

For the flood risk modeling analysis, six datasets were systematically selected and adapted to the specific environmental and geographical conditions of Ulaanbaatar, drawing from internationally validated methodologies employed in comparative urban flood risk assessments. The initial analytical phase involved the transformation of all spatial datasets into a coordinate system appropriate for Mongolia using advanced spatial analysis software, with each thematic layer developed to ensure geometric and radiometric consistency across the analytical framework.

Given the heterogeneous nature of measurement units across the diverse datasets, the Analytic Hierarchy Process (AHP) methodology was employed to facilitate comparative analysis and establish appropriate weighting schemes for multi-criteria evaluation. The AHP is a structured technique for organizing and analyzing complex decisions, based on mathematics and psychology, developed by Thomas L. Saaty in the 1970s (Saaty, 1977). The AHP is a theory of measurement through pairwise comparisons and relies on the judgements of experts to derive priority scales that measure intangibles in relative terms (Saaty, 2008). This methodology has been extensively validated in contemporary flood risk assessment applications, with recent studies demonstrating its effectiveness in coupling GIS mapping capabilities with AHP Decision-Making resulting from paired comparison matrices of expert groups (Mourato et al. 2023).

The AHP methodology facilitates the systematic determination of relative weights for multi-criteria decision-making through pairwise comparison matrices. The AHP is based on paired comparisons and employs hierarchical structures to depict a problem and then establish priorities for alternatives based on the user's assessment (Saaty, 1980). The fundamental principle underlying this approach involves the calculation of suitability indices expressed through the following mathematical framework:

$$S = \sum (W_i - F_i) , \qquad (1)$$

where S = Suitability index of the evaluated object

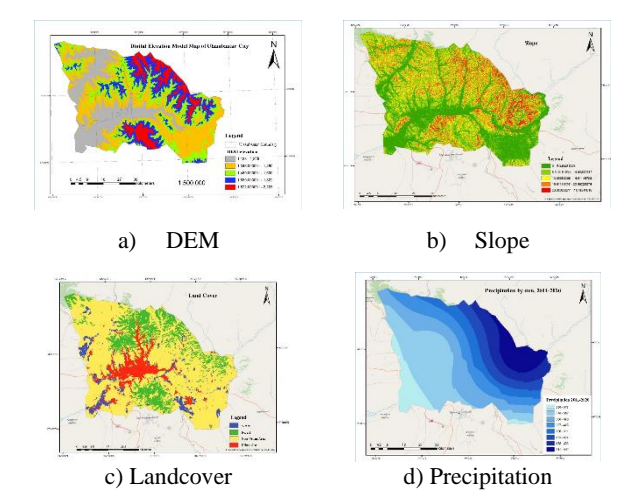
 W_i = Weighted coefficient of factor i

 F_i = Normalized criterion factor score for factor i

The hierarchical ranking methodology involves systematic comparison of research factors, determining their relative influence on flood risk indicators through percentage-based weighting schemes. The AHP method is used to obtain an optimum solution for a complex problem in different areas of science by weighing the variables (Saaty, 1980). The pairwise comparison approach utilizes a standardized numerical scale ranging from 1 to 9, where 1 represents equal importance and 9 indicates extreme importance of one criterion over another (Saaty, 1980).

Input data	Accuracy	Source	
Digital elevation	12.5 m	Digital elevation	
map		images from	
		"ALOS/PALSAR"	
		(https://search.asf.alas	
		<u>ka.edu/)</u>	
	30 m	Channel 11 data from	
		Landsat 8	
		(https://earthexplorer.	
		usgs.gov/).	
	10 m	The 2022 land cover	
		image from "ESRI	
		Sentinel-2 Land Cover	
		Explorer"	
Precipitation	90 m	Precipitation data	
		from 2011-2020 from	
		"Version 4 of the	
		CRU TS monthly	
		high-resolution	
		gridded multivariate	
		climate dataset".	

Table 1. Summary of data used in the study







e) Watershed f) Hydr Figure 4. Data and dataset

The process involved generating thematic layers from the input data (see Table 1 and Figure 4), ranking them according to their relative importance, and computing the weight of each element (Table 2) using threshold values derived from AHP analysis (Saaty, 2008). The AHP methodology facilitated a structured comparison of criteria, ensuring a systematic evaluation of their contributions to the overall decision-making framework.

ID	Input data	Importance	Rank
1	Land use	0.10	6
2	Digital elevation map	0.20	3
3	Hydrology flow/stream directions	0.25	1
4	Slope	0.21	2
5	Precipitation	0.11	5
6	Water basin	0.13	4

Table 2. AHP analysis of input data

4. Results

Flood risk is fundamentally determined by the interaction between hazard and vulnerability, where hazard represents environmental exposure to flooding and vulnerability reflects socio-economic susceptibility to its impacts. These components are not inherently correlated — a region may exhibit low flood hazard but high socio-economic vulnerability, or conversely, high hazard but low vulnerability. Consequently, comprehensive risk analysis necessitates the integrated assessment of both factors.

Flood risk mapping synthesizes multiple geospatial and climatic parameters, including:

- Land use/land cover (e.g., impervious surfaces, vegetation density)
- Topographic attributes (elevation, slope gradient, flow accumulation)
- Hydrometeorological data (precipitation intensity, return intervals)
- Hydrographic features (watershed boundaries, drainage density)

As shown in figure 5, the spatial integration of these variables through weighted overlay analysis generates a probabilistic flood risk zonation framework, enabling the formulation of differentiated mitigation strategies informed by localized

interactions between hazard and vulnerability factors. The spatial analysis of the flood risk map identified significant geographic patterns in hazard distribution. The highest flood risk concentrations occur in two distinct geomorphological contexts: (1) riparian zones adjacent to the Tuul River floodplain, and (2) piedmont areas along the foothills of Bogd Khan mountain. Quantitative assessment revealed that very high-risk zones encompass 775.7 km² (19.66% of the study area), while high-risk areas cover 1006.89 km² (25.5%), as detailed in table 3. These risk concentrations reflect the compounding effects of hydrological forcings (riverine overflow potential) and topographic controls (steep-gradient runoff accumulation).

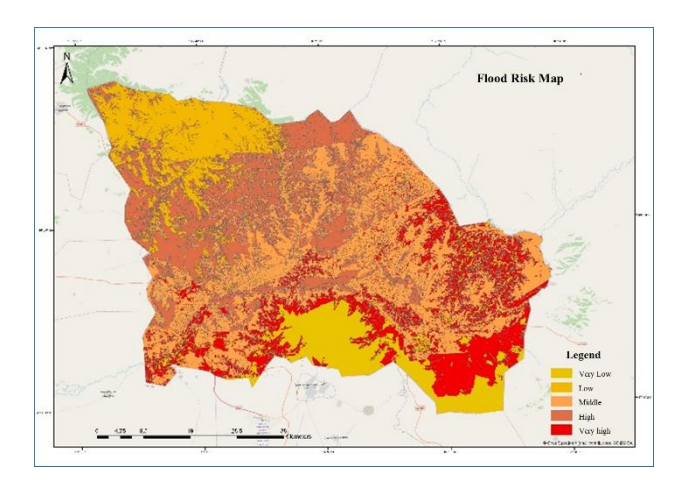


Figure 5. Flood risk map

Flood hazard level	Area size (km2)	Percentage (%)
No Risk	446.7	11.3
Low Risk	497.9	12.6
Medium Risk	1218.8	30.9
High Risk	1006.9	25.5
Very High Risk	775.7	19.7

Table 3. Flood risk areas

The flood risk assessment reveals distinct spatial patterns across Ulaanbaatar's administrative districts. Three districts exhibit particularly severe exposure: Nalaikh, Bayanzurkh and Khan-Uul are classified within the very high-risk category. Concurrently, Sukhbaatar, Songinokhairkhan and Chingeltei districts demonstrate elevated but marginally lower risk levels, falling within the high-risk classification (Figure 6). This spatial distribution correlates strongly with topographic features and hydrological networks, where lower-lying districts and those intersecting major watersheds demonstrate greater flood susceptibility.

The analysis identifies 775.7 km² of very high flood risk areas encompassing multiple administrative units across three districts. The affected areas include:

- Khan-Uul district: All khoroo (sub-districts) fall within this highest risk category
- Bayanzurkh district: Six specific khoroo (3rd, 15th, 18th, 1st, 6th, and 11th)
- Nalaikh district: Three khoroo (3rd, 5th, and 6th)

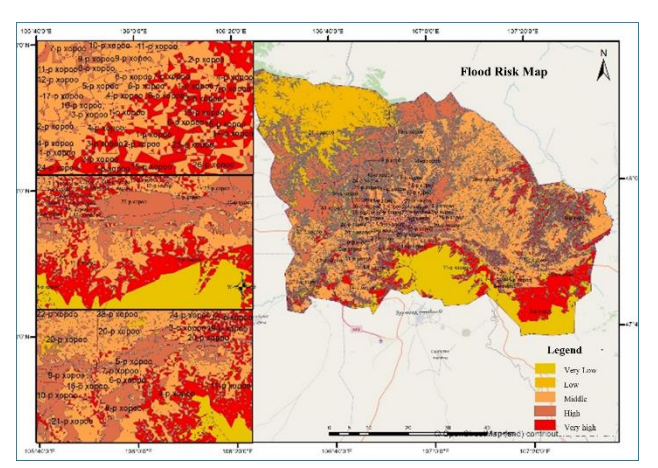


Figure 6. Subdistricts in high flood risk areas

These high-risk zones are documented in table 4, which provides detailed spatial and administrative breakdowns. The concentration of risk in these particular khoroo suggests significant vulnerability due to a combination of topographic, hydrological, and possibly urban development factors.

Risks	Districts	Khoroo	Area	Percentage
			(km ²)	(%)
Very	Khan-Uul	The Khoroo	1006.9	25.52
High		listed—3, 4,		
		6, 8, 9, 10,		
		11, 12, 14,		
		16, 18, 19,		
		20, and 21—		
		are located in		
		areas with		
		very high		
		flood risk.		
	Bayanzurkh	The Khoroo		
		listed— 1, 3,		
		6, 11, 15, and		
		18 — are		
		located in		
		areas with		
		very high		
	NT-1-11-1	flood risk.		
	Nalaikh	The Khoroo		
		listed— 3, 5, and 6—are in		
		areas with		
		very high		
		flood risk.		
High	Songinokhairkhan	The Khoroo	775.7	20.0
mgm	Bongmoknanknan	listed— 1, 8,	775.7	20.0
		9, 10, 21, 25,		
		26, 33, 34,		
		35, 36, 40,		
		and 42—are		
		in areas with		
		high flood		
		risk.		
	Chingeltei	All khoroo		
	Sukhbaatar	are in areas		
		with high		
		flood risk.		
	Bayanzurkh	The Khoroo		
		listed—		
		2, 3, 5, 6, 11,		
		14, 16, 18,		
		21, 22, 24,		
		27, and 28—		
		are		

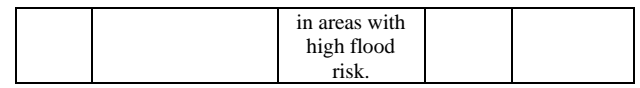


Table 4. Districts and subdistricts in flood risk areas

5. Conclusion

The Analytic Hierarchy Process (AHP) was employed following a systematic evaluation of alternative flood risk assessment techniques, including hydrological modeling, hydraulic simulations, and rainfall-runoff analyses. This decision was driven by AHP's capacity to integrate and quantitatively compare heterogeneous geospatial datasets through pairwise criteria evaluation, enabling a robust multi-parametric assessment of flood susceptibility factors.

Thematic layers were derived from ALOS PALSAR synthetic aperture radar (SAR) digital elevation models at 12.5 meter resolution, incorporating terrain parameters critical to flood modeling: elevation gradients, slope aspect, flow accumulation, and watershed boundaries. These processed layers serve dual purposes: as foundational inputs for hydrodynamic simulations and as standalone datasets for geomorphological studies, particularly in analyzing erosion patterns and land degradation susceptibility across variable topographies.

The AHP derived flood risk matrix categorized the study area into five ordinal risk classes:

- Very High-risk zones (775.7 km², 21.3% of study area)
- High-risk zones (1006.89 km², 27.6%)
- Moderate-risk zones (1218.7 km², 33.4%)
- Low-risk zones (446.7 km², 12.2%)
- No risk zones

Spatial analysis identified concentrated vulnerability in specific administrative units, particularly Khan-Uul District's 14th, 16th, and 19th khoroo, where alluvial fan morphology exacerbates flood propensity. A 32.8 hectare land-use audit in District 32 quantified exposure magnitudes: 73.2% residential land cover, 7.3% impervious surfaces (buildings/roads), and 6.1% critical infrastructure exhibited high inundation susceptibility.

A three-dimensional cadastral unit model was integrated with the flood risk matrix through geostatistical overlay analysis. Scenario testing at incremental water surface elevations revealed nonlinear exposure growth:

- Dund Dari Eh: 1.0 m stage affected 7 units (4.8 ha), escalating to 27 units (18.3 ha) at 2.0 m
- Nogoon Nuur: 1.5 m stage impacted 21 units (14.7 ha), doubling to 36 units (25.2 ha) at 2.0 m

The differential vulnerability between sectors reflects variations in urban density, drainage infrastructure capacity, and topographic confinement ratios.

References

Abou Rjeily, Y., Abbas, O., Sadek, M., Shahrour, I., Hage Chehade, F., 2017: Flood forecasting within urban drainage systems using NARX neural network. *Water Science and Technology*, 76(9-10), 2401–2412. https://doi.org/10.2166/wst.2017.409

Al-Omari, A., Al-Qinna, M., Elkhrachy, I., Elbashir, M. A., Hamad, L., Al-Fugara, A., & Alobeiaat, A., 2024: Utilizing remote sensing and GIS techniques for flood hazard mapping and risk assessment. *Civil Engineering Journal*, 10(4), 1203–1222. https://doi.org/10.28991/CEJ-2024-010-04-08

Amatebelle, C.E., Owolabi, S.T., Ogundeji, A.A., Okolie, C.C., 2025: A systematic analysis of remote sensing and geographic information system applications for flood disaster risk management. *Journal of Spatial Science*. https://doi.org/10.1080/14498596.2025.2476973

Asian Development Bank, 2018: Can better urban planning help Ulaanbaatar glimpse a brighter future? https://www.adb.org/results/can-better-urban-planning-help-ulaanbaatar-glimpse-brighter-future

Batimaa, P., Myagmarjav, B., Batnasan, N., Jadambaa, N., Khishigsuren, P., 2011: *Urban water vulnerability to climate change in Mongolia*. United Nations Environment Programme. https://wedocs.unep.org/20.500.11822/7941

Bruno, L.S., Mattos, T.S., Oliveira, P.T.S., Almagro, A., Rodrigues, D.B.B., 2022: Hydrological and hydraulic modeling applied to flash flood events in a small urban stream. *Hydrology*, 9(12), 223. https://doi.org/10.3390/hydrology9120223

Chebotarev, A. I., 1975: *Hydrological dictionary* (3rd ed.). Gidrometeoizdat.

Chen, J., Hill, A.A., Urbano, L.D., 2009: A GIS-based model for urban flood inundation. *Journal of Hydrology*, 373(1–2), 184–192. https://doi.org/10.1016/j.jhydrol.2009.04.021

Chen, Y., Zhou, H., Zhang, H., Du, G., Zhou, J., 2020: How does increasing impervious surfaces affect urban flooding in response to climate variability? *Ecological Indicators*, 117, 106613. https://doi.org/10.1016/j.ecolind.2020.106613

Climate and Clean Air Coalition, 2024: Mongolia increases climate change ambition with actions that improve air quality and human health. https://www.ccacoalition.org/news/mongolia-increases-climate-change-ambition-actions-improve-air-quality-and-human-health

Climate Change News, 2022: Mongolia flood defence project shows the way for urban adaptation. https://www.climatechangenews.com/2022/05/12/mongolia-flood-defence-project-shows-the-way-for-urban-adaptation/

Dysarz, T., Wicher-Dysarz, J., Sojka, M., 2023: Integrated hydraulic-hydrological modeling for flood risk assessment: Methodological frameworks and case studies. *Water Resources Research*, 59(3), e2022WR033871. https://doi.org/10.1029/2022WR033871

Farhadi, H., Najafzadeh, M., 2021: Flood risk mapping by remote sensing data and random forest technique. *Water*, 13(21), 3115. https://doi.org/10.3390/w13213115

Gordillo Fuertes, E., 2023: Understanding contemporary challenges for water security in Ulaanbaatar, a semi-arid region in Mongolia. *PLOS Water*, 2(12), e0000160. https://doi.org/10.1371/journal.pwat.0000160

Hagos, Y.G., Andualem, T.G., Yibeltal, M., 2022: Flood hazard assessment and mapping using GIS integrated with multi-criteria decision analysis in upper Awash River basin, Ethiopia. *Applied Water Science*, 12, 148. https://doi.org/10.1007/s13201-022-01674-8

Intergovernmental Panel on Climate Change, 2022: *Climate change 2022: Impacts, adaptation and vulnerability*. Cambridge University Press. https://www.ipcc.ch/report/ar6/wg2/

Intergovernmental Panel on Climate Change, 2023: *AR6* synthesis report: Climate change 2023. https://www.ipcc.ch/report/ar6/syr/

Khatooni, K., Hooshyaripor, F., MalekMohammadi, B., Noori, R., 2025: A new approach for urban flood risk assessment using coupled SWMM-HEC-RAS-2D model. Journal of Environmental Management, 374(123849), 123849. https://doi.org/10.1016/j.jenvman.2024.123849

Kumar, V., Sharma, K.V., Caloiero, T., Mehta, D.J., Singh, K., 2023: Comprehensive overview of flood modeling approaches: A review of recent advances. *Hydrology*, 10(7), 141. https://doi.org/10.3390/hydrology1007014

Li, Y., Wang, X., Chen, L., Zhang, M., 2025: Sustainable stormwater management: Runoff impact of urban land layout with multi-level impervious surface coverage. *Sustainability*, 17(8), 3511. https://doi.org/10.3390/su17083511

Maidment, D. R. (Ed.)., 1992: *Handbook of hydrology*. McGraw-Hill.

Ministry of Environment and Tourism, 2023. *Climate characteristics of Mongolia*. Government of Mongolia.

Mourato, S., Fernandez, P., Pereira, L.G., Moreira, M., 2023: Assessing vulnerability in flood prone areas using Analytic Hierarchy Process—Group Decision Making and Geographic Information System: A case study in Portugal. *Applied Sciences*, 13(8), 4915. https://doi.org/10.3390/app13084915

NASA, 2024: Extreme weather and climate change. NASA Climate Change and Global Warming. https://science.nasa.gov/climate-change/extreme-weather/

National Statistics Office of Mongolia, 2022: Classification and share of the unified land fund of the capital city. Government of Mongolia.

Saaty, T.L., 1977: A scaling method for priorities in hierarchical structures. *Journal of Mathematical Psychology*, 15(3), 234–281. https://doi.org/10.1016/0022-2496(77)90033-5

Saaty, T.L., 1980: The analytic hierarchy process: Planning, priority setting, resource allocation. McGraw-Hill.

Saaty, T.L., 2008: Decision making with the analytic hierarchy process. *International Journal of Services Sciences*, 1(1), 83–98. https://doi.org/10.1504/IJSSCI.2008.017590

UNICEF Mongolia, 2024: *Climate change and air pollution*. https://www.unicef.org/mongolia/environment-air-pollution

World Bank, 2020: Guidebook on capital investment planning for the capital city of Ulaanbaatar. https://documents1.worldbank.org/curated/en/87160158644330 0364/txt/Guidebook-on-Capital-Investment-Planning-for-the-Capital-City-of-Ulaanbaatar.txt

WWF, 2024: *A healthy Tuul River for Mongolia*. https://www.worldwildlife.org/projects/a-healthy-tuul-river-formongolia